IAC-20-A2.3.4

Leveraging Microgravity to Investigate Earth- and Space-Based Centrifugal Casting of Wax

Keith Javier Stober[a]*, Alana Sanchez[b], M. Regina Apodaca M.[c], Gladys Ngetich[a], Daniel Erkel[c], Juliet Wanyiri[a], and Danielle Wood[ac]

[a] *Media Lab, Massachusetts Institute of Technology, 77 Massachusetts Ave., Cambridge, Massachusetts 02139, USA, stober@mit.edu, gladysn@mit.edu, jwanyiri@mit.edu, drwood@media.mit.edu*
[b] *Department of Physics, Massachusetts Institute of Technology, 77 Massachusetts Ave., Cambridge, Massachusetts 02139, USA, asanchz@mit.edu*
[c] *Aeronautics and Astronautics, Massachusetts Institute of Technology, 77 Massachusetts Ave., Cambridge, Massachusetts 02139, USA, mapodaca@mit.edu, derkel@mit.edu*
* Corresponding Author

Abstract

A multi-year research effort aimed at increasing understanding of the centrifugal casting process of wax fuels for hybrid chemical propulsion in multiple thermal and gravitational environments is described. As both radiative and convective heat transfer drive the casting process, the suborbital and orbital microgravity environments are critical to disentangling these contributions to heat transfer away from the fuel. The experimental effort comprises testing on multiple platforms, including the ambient atmosphere of the laboratory, as well as various mobile microgravity platforms. Testing onboard reduced-gravity aircraft facilitates increased understanding of how these types of fluids perform in the microgravity environment, while a suborbital spaceflight and orbital platform under standard atmosphere allow for longer-term observation of natural convection sans buoyancy. An orbital platform subjected to the space environment facilitates understanding of the contribution of radiation to the heat transfer away from the liquid fuel. Each progressive testing environment requires updates to the experimental setup in order to accommodate respective physical and electrical constraints which are described in detail herein. An image analysis routine was developed in order to automate post-processing and determine the solidification front speed for each test. A rotation rate actuation routine is in development which aims to improve the accuracy of the centrifuge control system by leveraging electromagnetic sensing and feeding back rotation rate measurements to the motor driver. Preliminary modeling work was conducted which aims to elucidate the fundamental physics of the centrifugal casting problem; specifically, the impact of rotation rate, material properties, and environmental conditions on the heat transfer and fluid mechanics which constitute the larger casting problem. Both paraffin wax -- a solid fuel with two decades of heritage -- and the more novel beeswax are considered in this study.

Keywords: Green propellants, hybrid chemical propulsion, wax

Acronyms/Abbreviations
PCM   phase change material
RPM   revolutions per minute
fps   frames per second

1. Introduction

The advent of paraffin-based hybrid chemical propulsion marked by the doctoral investigations of Karabeyoglu et al. in the late 1990's catalyzed widespread interest in wax fuels and the auxiliary technologies which facilitate their use [1]. The development of Peregrine, a paraffin-based suborbital rocket capable of lifting 5 kg to 100 km altitude and the selection of a paraffin-based chemical propulsion system as a finalist for the Mars Ascent Vehicle indicate the degree to which wax-based fuels have matured [2, 3]. There is a notable absence of literature, however, on efforts which consider the use of wax fuels for in-space chemical propulsion systems, despite the fact that paraffin waxes have been used for decades as phase change material (PCM) thermal regulators onboard satellites [4]. The research effort described herein attempts to address this gap by seeking a deeper understanding of the in-orbit centrifugal casting process -- a process which would enable in-situ fabrication of fuel grains and, of particular interest, the re-use of wax PCM as a fuel for deorbit of a small satellite. The centrifugal casting process comprises the melting of wax, the rapid rotation of the casting tube enveloping the wax to form an annulus (or tube), and the gradual solidification of the wax as heat escapes the casting tube, thereby lowering the wax temperature below its solidification point of 65-69 °C. Casting has been studied extensively in 1g, but much less in microgravity. It is hypothesized that

forming an annulus in liquid wax would be easier in microgravity due to wall friction being the only dominant force on the wax. However, the possibility also exists that in the absence of gravity, the wax may slip along the walls of the casting tube, thereby making annulus formation more challenging.

The work presented herein is a continuation of research efforts described previously by the authors [5-8]. Reference [5] established the ignition properties of paraffin wax and derivatives as compared to state-of-the-art satellite propellants, yielding encouraging results which merited further investigation of paraffin for in-space propulsion. In the remaining prior works, the results of two reduced-gravity aircraft flights are presented, as well as an extensive literature review of beeswax as a fuel for hybrid chemical propulsion. Detailed discussions of the experimental setup development and specifications were also reported. Annulus viability and rotation rate are key performance metrics for the system; comparisons between 1g and microgravity, as well as between different working fluids and casting tube geometries were presented. The overarching research effort is presented in Fig. 1. This figure displays the major steps involved in the research process conducted by the authors, as well as parallel work by other investigators which feeds into the studies described herein. Some of these steps are fundamental,

while others are applied. Ultimately, this research plan seeks to build off of prior studies in the area of fluid mechanics, heat transfer, and wax-based rocket propellants in order to more comprehensively understand the centrifugal casting process of wax on Earth and in microgravity.

This research looks at both paraffin and beeswax as working fluids because paraffin has been investigated as a high-performing hybrid rocket fuel for two decades and beeswax shows promise as a renewable fuel with material properties and performance on par with paraffin. For an in-depth literature review of beeswax as a fuel for hybrid chemical propulsion systems, see Ref. [8].

2. Technical Approach

The research effort comprises experimental as well as numerical approaches to understanding centrifugal casting described here.

2.1 Experimental Platforms

In order to understand the fluid mechanics and heat transfer mechanisms driving the centrifugal casting process, various experimental environments are employed which isolate the contributions of convection and radiation to heat transfer. Figure 2 shows the experimental environments which are expected to be employed as part of the larger research effort.
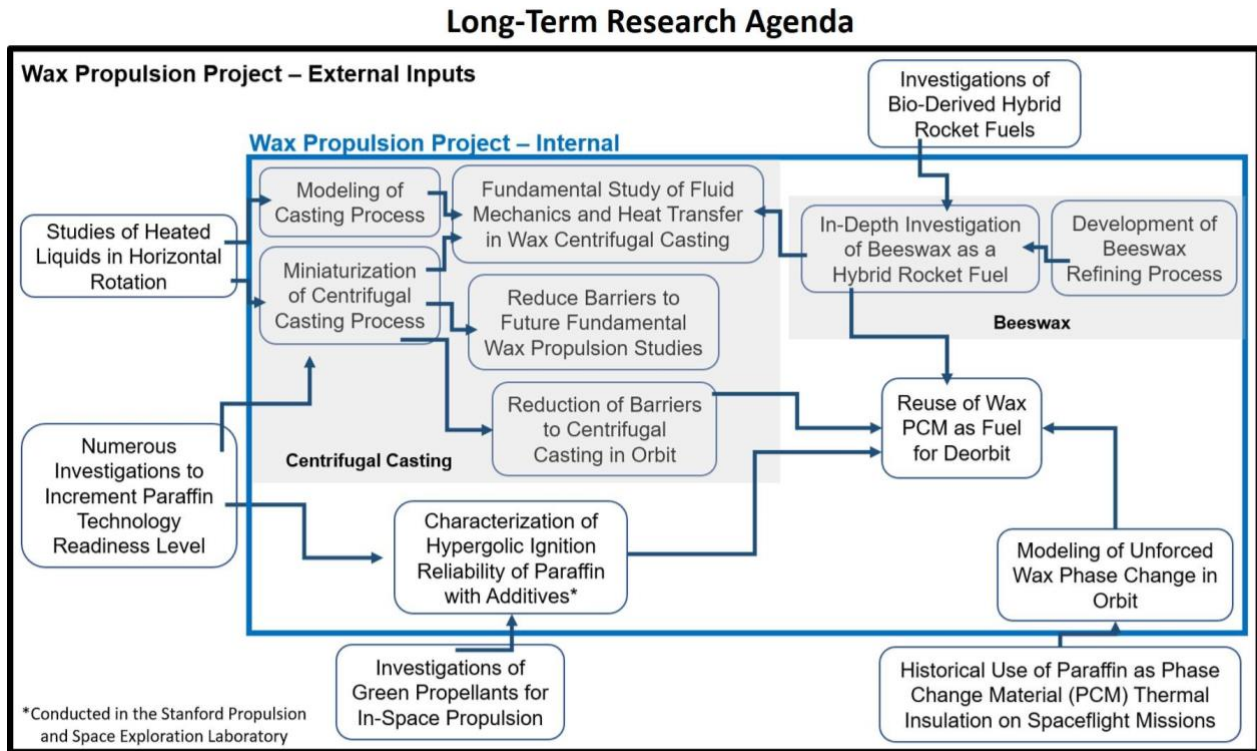

Fig. 1. Overarching research agenda incorporating inputs from prior work in the areas of green propellants for in-space propulsion, beeswax and paraffin performance characterizations, and thermal/fluid modeling of heated liquid in horizontal rotating cylinders.

2.1.1 Laboratory

A tabletop apparatus provided a highly-controlled environment to run all initial tests and improve experimental methods. Various casting tube diameter, lengths, and control mechanisms were tested and the image analysis routine was refined. In addition to the tabletop experiment in standard atmosphere, a vacuum chamber will be leveraged to better understand 1g radiative heat transfer out of the liquid-filled casting tube.

2.1.2 Reduced-Gravity Aircraft

Experiments conducted onboard ZeroG Corporation's parabolic-trajectory aircraft allow for short-term microgravity -- approximately 20 parabolas of 20 seconds each -- which is an ideal environment for proof-of-concept experiments as well as acquisition of preliminary results which inform future long-term microgravity experimental designs. To date, two of these flights have been conducted -- one each leveraging water and oil as working fluids in October 2018 and August 2019, respectively -- and aided in understanding the relationship between motor driving voltage and rotation rate as compared with the 1g case. As was hypothesized, lower rotation rates are required to form an annulus in both water and oil in microgravity versus identical conditions in the laboratory. Two more flights are upcoming which will leverage paraffin and beeswax. These flights present an engineering challenge as they will require in-situ heating and melting of wax. A heater is necessary to melt the wax and implementing a system which applies heat to a rotating cylinder is a challenge. A slip ring is ultimately required to accomplish this task, though the slip ring adds weight and structural complexity. These flights will also employ four centrifuges within one experimental rig, as shown in Fig. 3. In general, reduced-gravity aircraft flights facilitate investigation of the fluid mechanics of the centrifugal casting process, while longer-term microgravity platforms facilitate investigation of the heat transfer phenomena associated with that same process.
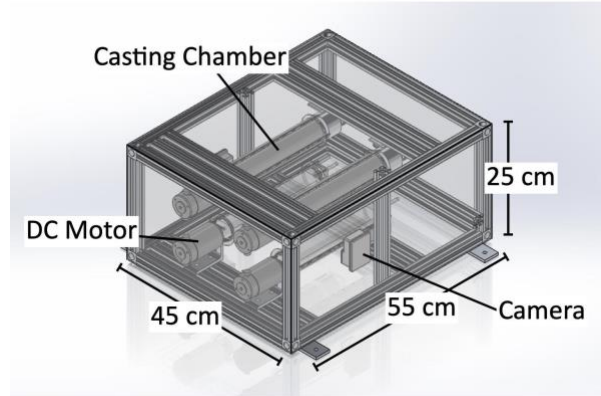

Fig. 3. Experimental setup for the third flight onboard a reduced-gravity aircraft comprising four parallel centrifugal casting tubes as opposed to prior tests which exhibited only one. Water, oil, paraffin, and beeswax will be leveraged as working fluids.

2.1.3 Suborbital Spaceflight

Two upcoming flights are scheduled onboard the Blue Origin New Shepard vehicle which facilitates a suborbital flight to over 100 km altitude yielding three continuous minutes of microgravity time. A constraint of this experimental setup is the considerably smaller form factor. Considering the small satellite volume standard of 1U = 10x10x10 cm^3, the first two reduced-gravity aircraft flights exhibited 48U volumes, while the suborbital flight is limited to 2U. Fig. 4 displays a solid model of the experimental configuration for the suborbital flight.
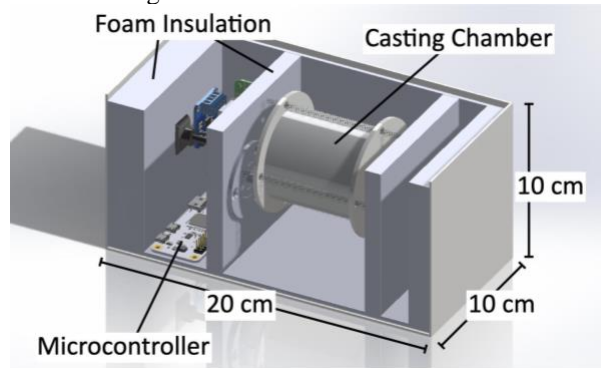

Fig. 4. Experimental setup for centrifugal casting onboard the Blue Origin New Shepard suborbital spaceflight comprising typical hardware of prior centrifugal casting processes with the additional elements of a more advanced microcontroller and imaging setup.

2.1.4 Orbital Platforms

In order to run complete centrifugal casting cycles, from solid to liquid to annulus formation and resolidification, a long-term microgravity environment will be required. Ideally, such an orbital platform would

Fig. 2. Various experimental platforms which facilitate the isolated understanding of different gravitational and thermal impacts on the centrifugal casting process.

provide both a standard atmosphere to test the influence of convection in the absence of gravity and a platform with exposure to the space environment of low Earth orbit. The Space Enabled Research Group is in the process of conceptual design for an experiment on such a platform.

2.2 Rotation Rate Control

When talking about a rotation rate control, it is referring to the ability to properly measure and control the rotation speed of the motor that is used to run the centrifuge. This is especially important since a main component of this study is to understand the relationship between rotation speed of the centrifuge and the quality of the casted annulus. Including a rotation rate control is a necessary improvement given the nature of microgravity experiments. would improve the precision of this study since it would allow for a more accurate measurement and control of rotation speed.

The partial and temporary removal of the gravitational forces when running the different experiments described in this paper in microgravity flights, causes there to be an inconsistency in the RPM of the centrifuge at a given voltage. This same behaviour can be expected when carrying out these experiments in rocket flight and ISS flights. That is why the inclusion of a new RPM sensor that is calibrated while the experiment is in microgravity would allow the relationship between the RPM and the voltage being applied to the motor to be properly and more precisely characterized.

There are multiple considerations to be made when designing a rotation rate controller. The first one being the limitation in weight and space that these experimental beds have. Ideally, it would be possible to include the controller in the already existing experimental setups, as well as a simple consideration for future iterations. Secondly, given the presence of multiple reflective surfaces and the lack of control over the lighting of the experiment, it is believed that a light-based sensor would not be convenient for the described experiment. Therefore, a magnetic sensor or a sensor that uses the hall effect, is proposed for the rotation rate controller. The hall effect is when a conductor through which one applies an electric current, experiences an induced voltage difference perpendicular to that being applied, when brought close to a magnet. For the use of this sensor to measure the RPM of the centrifuge, a magnet must be attached to the rotating body. When doing so, it is important to keep multiple things in mind such as the distance from the sensor and the size of the magnet.

As previously mentioned, the design selected for the rotation rate control system consists of a motor, a magnetic sensor and an adapter piece that mounts onto the motor shaft and in which we place both the casting tube and the magnet. On Figure 5 we see the motor adaptor piece, along with the magnet and the sample

aluminium tube. The sensor is connected to an arduino which is used to collect the readings and control the motor. This sensor is connected via a breadboard that is placed at 2.5mm from the first magnet slot.

Fig. 5. Rotation Rate controller set. On the top Figure, we see the side view of the test setup. Here we see how the motor mount is attached to the motor shaft. The aluminium tube is also attached to the Motor Mount. The bottom image is the frontal view of the motor mount. On the bottom right, we can see the small magnet that has been placed in one of the side slots.

Moreover, the design of the mount allows for the testing of three different sizes of magnets and for placing the magnet at different radial distances (see figure). This allows for the testing of the influence both the distance of the magnet from the detector and the size of the magnet may have on the precision of the RPM detection. Both the motor and the sensor are operated using Arduino Uno.
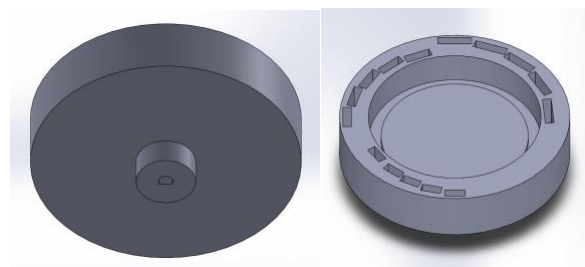

Fig. 6. Motor Mount 3D printed part. This piece attaches to the motor shaft. The curvilinear rectangular holes are to test different radial distance and magnet size.

2.3 Image Analysis

In order to analyze the behavior of paraffin wax and beeswax in the centrifugal casting chamber, an image analysis script was created in Python to track the rate of solidification of both waxes. This script is able to track the solidification process in any environment, both in the lab and in microgravity, as long as there is video available that displays the solidification over time. The rate of solidification describes the response of the wax within the centrifugal casting chamber and the length of time needed to reach full solidification. Determination of expected solidification time is especially important in situations with tighter temporal constraints, such as choosing the optimal material to use for casting on a microgravity flight with less than 20-180 seconds of continuous reduced gravity.

Two videos were taken with a GoPro HERO 7 Black with a frame rate of 60 frames per second (fps) over the full length of solidification for both paraffin wax and beeswax. Individual frames were binarized and the differentiated boundary between the liquid and solid wax was tracked. Further analysis showed that with the high volume of available frames and the slow solidification rate that using only one fps did not affect the accuracy but did significantly reduce computational time.

There remains some ambiguity in the choice of solidification front due to the presence of multiple phases in the solidification process. For the purposes of this project, the leading edge of solidification, defined as where the liquid wax meets the partially solidified (semisolid) wax boundary, was chosen to represent the front of solidification rather than the boundary between the semisolid and solid wax layer due to the former being a clearer boundary for use with the Python binarization script. Both the leading and trailing edge of solidification can be seen in Figure 7 observed over the solidification process of paraffin wax. The presence of two solidification fronts is particularly evident in beeswax due to the large variety of chemical constituents, over 300, which result in varying melting temperatures within the wax [9, 10, 11]. The clarity in solidification fronts in beeswax reduces noise in the image analysis process when compared to paraffin wax.
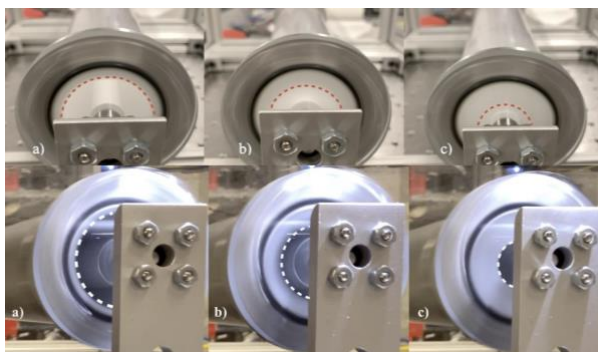

Fig. 7. The centrifugal casting and solidification process for paraffin wax, depicting both the trailing (red dashed line) and leading (white dashed line) solidification front migrating radial inwards.

The Python script is also optimized to manually select the region of solidification, allowing for increased flexibility in where the camera can be placed in-lab. A conversion factor to convert pixels to a physical distance was obtained using the width of the o-ring groove on the face of the solidification chamber. The o-ring groove can be seen as the first black band of each frame in Figure 8 along with the process of solidification over 12 frames spaced 1 minute apart. The white region following the o-ring groove consists of both an aluminum lip and solidified wax. This aluminum lip was treated as a constant factor and subtracted from the final solidification process to fully depict the solidification of only the wax. Complete solidification in Figure 8 occurs at approximately 10 minutes, depicted by the tenth frame.
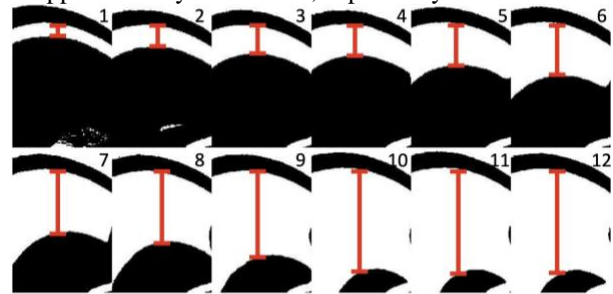

Fig. 8. Solidification process of beeswax (encased within the red line region) in the solidification chamber shown as a series of binarized frames spaced 1 minute apart over 12 minutes.

3. Results

3.1 Image Analysis

Solidification analysis for laboratory tests of both beeswax and paraffin wax yielded two solidification curves as well as an analysis of their instantaneous solidification rate and can be seen in Figure 9. Due to the distinct color difference between solid and liquid beeswax, where newly solidified beeswax appears light yellow and liquid beeswax appears medium brown, the image analysis script experienced a reduction in error when tracing the solidification distance of the beeswax. The two dips in the solidification process of beeswax are the result of a momentary spin up and spin down of the driving DC motor that results in a remelting of the wax in both cases.

The tracking of solidification distance for paraffin wax experienced more errors due to the relative transparency of liquid paraffin wax and the tendency of the wax to diffuse light resulting in varying ambient lighting conditions in the chamber. This inconsistency in lighting increased the error when accounting for

solidification distance and required the division of the solidification process into two different regions. The solidification for the first 6 minutes of paraffin utilized a horizontal distance tracking procedure and the subsequent solidification utilized a vertical procedure. Due to the parallax caused by the acquisition setup, the data from the initial 6 minutes was scaled with a constant correction factor of 1.23 determined by the ratio of pixel-to-physical-distance conversion factors determined from the length of the o-ring groove mentioned previously.

As seen in Figure 9, beeswax completed solidification in approximately 22% less time than paraffin under identical initial conditions, despite covering 29% more distance due to coning on the ends of the chamber. This coning, defined as an increase in solidification distance on the end caps of the chamber when compared to the distance seen in the center of the chamber, resulted in a final external annulus diameter of 17 and 25 mm for beeswax and paraffin respectively rather than the ideal 25.4 mm. An example of coning can be seen in Figure 10, which depicts end responses in a paraffin fuel grain. The authors believe the presence of aluminum on either end, where the motor is connected to an aluminum end cap and the viewing chamber of the aft utilizes an aluminum ring to support the acrylic window, provided increased opportunity for heat to escape from the end caps when compared to the polycarbonate tube

and resulted in non-uniformities in the formation of annular diameter. The acrylic end cap exhibits a low thermal conductivity nearly identical to polycarbonate at 0.2 W/mK [12] and displays a favorable response when compared with other materials exhibiting high thermal conductivity. In a worst case scenario, the material of the end caps has zero thermal resistance and results in wax preferentially solidifying at the end caps and leaving a hollow cavity in the cross-sectional center of the chamber. The thermal response of the acrylic therefore much more closely matches the best case scenario, where high thermal resistance of the end caps results in identical annular cross sections throughout the fuel grain, even with the presence of some coning.
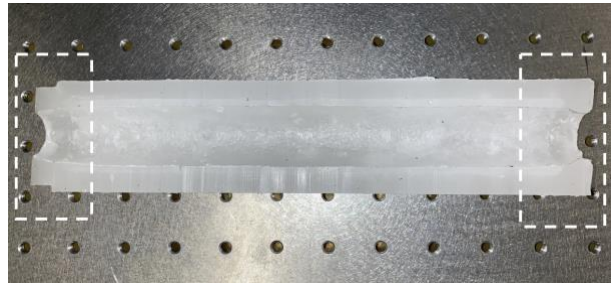

Fig. 10 Cross sectional view of a coning response in the ends of a paraffin wax fuel grain after centrifugal
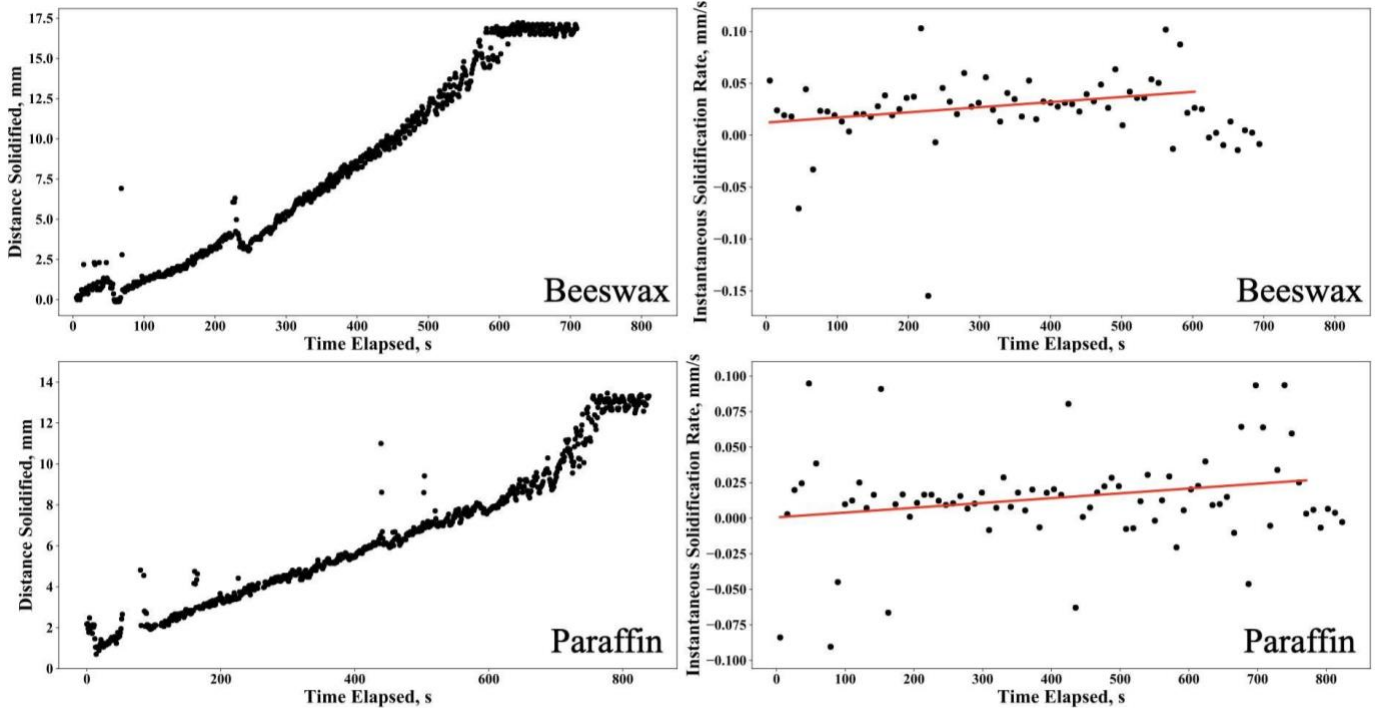

Fig. 9. Solidification process and instantaneous solidification rate analysis for a) beeswax and b) paraffin wax. Both tests were conducted in a 50.4 mm inner diameter, 254 mm length polycarbonate casting tube of 3.175 mm thickness and rotation rates exceeding 1500 rpm. Note the two dips in solidification of beeswax were caused by motor error and the increased noise in the solidification of paraffin was caused by ambient lighting effects unique to paraffin.

casting at 1850 rpm caused by an increase of heat escaping through the endcaps.

The total distance of solidification for beeswax is approximately 16.7 mm in 600 s compared to that of paraffin at 12.9 mm in 765 s, which results in a time- and space- averaged solidification rate of 0.028 and 0.017 mm/s for beeswax and paraffin, respectively. This determination indicates that even though the total distance solidified for beeswax was larger than paraffin, it still solidified completely more quickly than paraffin. This result indicates that for future microgravity flights where solidification is attempted and time is a constraint, beeswax could be a better option for centrifugal casting due to its larger solidification rate.

Instantaneous solidification rate was also determined in Figure 9 for both waxes between analyzed frames and binned by 10 to account for high noise exacerbated by a slow solidification rate and a large number of frames, making stepwise assertions of solidification distance difficult. A best fit line was included for the length of solidification and illustrates the gradual and steady increase in solidification rate over time. This result was surprising to the authors as the solidification rate increased with a smaller solid/liquid interface surface area through which heat can escape when compared to the beginning of solidification where heat is able to escape through a larger surface area. Solidified wax, however, exhibits an approximately 50% greater thermal conductivity than its liquid phase which accelerates the expulsion of heat from the center of the fuel grain. While these two phenomena contribute opposite effects on the solidification rate with time, it appears the latter effect was dominant and resulted in a solidification process that slightly accelerates with time.

4. Discussion and Future Work
4.1 Rotation Rate Control
The first step for the programming of the rotation rate controller was to output the measurements given by the sensor. An example of these graphs can be seen in Figure 11 where, when placed next to a rotating motor mount with the smallest the magnets (6mm diameter), at the shortest distance of 2.5 mm from the sensor and by applying a voltage of 1V to the motor, the oscillation and therefore frequency of the values is clear.
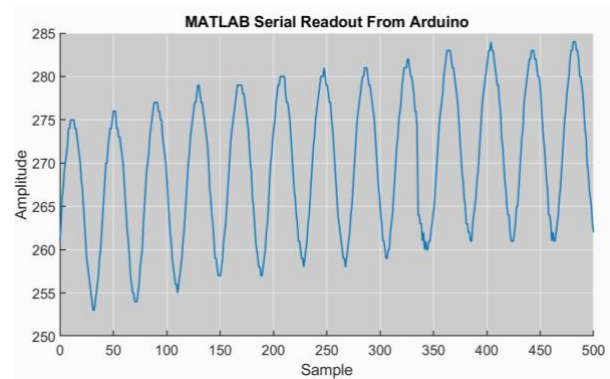

Fig. 11. Sinusoidal graph of the output amplitude versus the sample step given by the sensor when 1V voltage is applied to the motor.

Once it became evident the sensor was successfully measuring the rotation rate, the value of the RPM was therefore extracted. Since the accuracy and effectiveness of the sensor are being studied, it is necessary to have a second measuring device to compare the obtained values. This is done by simultaneously measuring the RPM with a commercially available optical tachometer and comparing it to the RPM reading given by the magnetic sensor. A discrepancy of approximately +20 RPM is identified between the optical tachometer and the one proposed by the authors. There are multiple possible explanations for this discrepancy, however, it is still too early to make any strong conclusions.

Additionally, an algorithm to allow for the calibration of the sensor is under development. The proposed methodology is to make a sweep of measured RPM versus applied voltages in order to identify a function that can be used by the motor to adjust the applied voltage to obtain the desired RPM.

For the purpose of this paper, only initial results of the rotation rate controller are shown given the delays caused by the COVID pandemic. In the future, the rotation controller will be redesigned to calibrate in the shortest time possible, given that the microgravity flights only allow for a very short experiment run time. Moreover, further work will explore the role played by the distance from the sensor, and the size of the magnet to influence the precision of the measurement.

4.2 Image Analysis
Image analysis of the solidification process of two centrifugal castings of paraffin and beeswax was conducted and resulted in measurements for the solidification distances and rates for each wax. These castings are in form factors congruent with small-scale hybrid rockets as part of this study's goal to facilitate the production of usable fuel grains onboard a satellite as an in-space propulsion system. An image analysis script was produced in Python to automate the measurement of

solidification through the acrylic end cap of the centrifugal casting chamber through the binarization of wax and the pixel-to-physical-distance conversion utilizing the o-ring groove visible on the aft of the chamber. Instantaneous solidification was analyzed from the solidification process resulting in a rate slightly but steadily increasing over time for both beeswax and paraffin wax. This acceleration is more apparent in beeswax and results in a faster solidification process than observed in paraffin. Coning was also observed on the ends of both fuel grains, though beeswax exhibited significantly more.

Future work will change the casting chamber from polycarbonate to aluminum which boasts a four-order-of-magnitude increase in thermal conductivity when compared with polycarbonate. The increase in thermal conductivity should decrease both casting time and coning in the resultant fuel grains. Further testing into the effect of the casting chamber length and diameter on the resultant fuel grains are also being tested in the lab.

Two future microgravity aircraft flights are currently planned to complement the two prior microgravity flights utilizing water and motor oil in the casting chamber. These upcoming flights will attempt to introduce an in-situ heating system to allow for both paraffin and beeswax to be viewed in the chamber. However, due to limitations on the length of periods of microgravity on the flight, it may not be feasible to perform solidification analysis.

An upcoming suborbital flight on the Blue Origin New Shepard vehicle is also planned to include liquid paraffin wax in a smaller casting chamber due to the 2U allowable volume for the entire experimental setup. Due to the increased length of sustained microgravity, on the order of 3 minutes, solidification analysis will be conducted on the paraffin fuel grain to produce an understanding of how the solidification process translates to a space-like environment.

4.3 Modeling

4.3.1 Future Modeling Work Overview

This section outlines future numerical modeling work. The numerical work, aside from validating the experimental work, will aid further understanding of fluid mechanics and heat transfer mechanisms of centrifugal casting of paraffin wax.
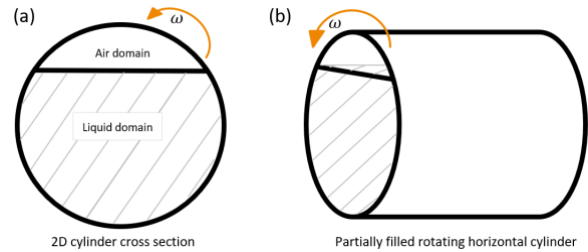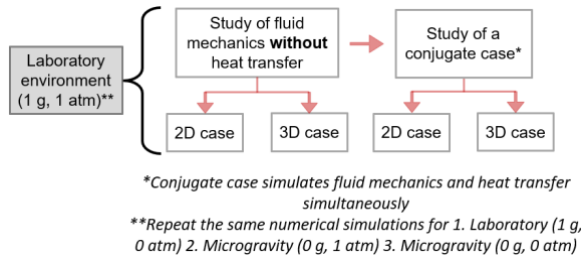

Fig. 12. (a) 2D cross sectional slice used for 2D simulation and (b) 3D horizontal cylinder used for 3D simulation

The numerical work will be subdivided into two major parts: 1. Study of fluid mechanics without heat transfer where CFD simulations will be carried out without heat transfer consideration. 2. Study of a conjugate case, where CFD simulates fluid mechanics and heat transfer simultaneously. For each of these two major cases, both 2D case and 3D case will be considered. See Figure 12 for simplified sketches of the 2D case and 3D case computational domains. The numerical work will focus on studying laboratory environment with 1 g and 1 atm conditions before increasing complexity into (1) laboratory with 1 g and 0 atm, (2) microgravity environment with 0 g and 1 atm and (3) microgravity environment with 0 g and 0 atm. In all these testing environments, Stober et al. outlines an assessment of the anticipated specific heat transfer mechanism contributions to the cooling and solidification process of wax centrifugal casting [8]. Table 1 gives a summarized outline of the numerical simulation work to be undertaken. The CFD numerical analysis will be undertaken using commercial CFD software ANSYS Fluent version 2020 R1.

Both experiments [6, 13] and numerical simulations [14] in literature have noted that liquid properties, such as density and viscosity, as well as rotating tube geometrical parameters such as tube length and tube diameter play a crucial role in the quality of the final cast product. The numerical work to be undertaken will also study the influence of these liquid properties and geometrical parameters on centrifugal casting. The results from these simulations will be important in the effort to design systems to perform centrifugal casting in microgravity. Table 2 gives some of the liquids as well as some of the important geometrical parameters that will be investigated.

Table 1. Paraffin wax centrifugal casting numerical simulation work plan summary

Conjugate case simulates fluid mechanics and heat transfer simultaneously
**Repeat the same numerical simulations for 1. Laboratory (1 g, 0 atm) 2. Microgravity (0 g, 1 atm) 3. Microgravity (0 g, 0 atm)*

4.3.2 Preliminary CFD Simulation and Results

This section presents preliminary results obtained by studying two liquids (water and SAE 15W-40 Motor oil) at three different rotational speeds (100 RPM, 1000 RPM and 2000 RPM) considering the laboratory test conditions (1 g and 1 atm). The liquids density and viscosity are as shown in Table 3. A 2D computational domain like that shown in Fig 12. (a) was considered.

Table 2. Liquid properties & geometrical parameters influence on centrifugal casting

Parameter	Value		
Liquid	Water	SAE 15W-40 Motor Oil	Paraffin Wax, Dotriacontane C32H66
RPM [-]	500	1000	2000
Tube Diameter [mm]	12.7	25.4	50.8
Tube Length [mm]	63.5	127.0	254.0

CFD simulations were performed in ANSYS Fluent version 2020 R1. All the simulations are transient permitting results visualization with time after post processing. Turbulence was modeled using Standard k-epsilon viscous model while multiphase modeling was achieved by employing Volume of Fluid (VOF) model. PISO discretization scheme was used for pressure-velocity coupling as it is recommended for transient flow

calculations [15]. PRESTO! Scheme was chosen for pressure spatial discretization as it is well suited for steep pressure gradients involved in most rotating flows. PRESTO! provides an improved pressure interpolation where there is presence of strong pressure variations, for instance in swirling flows. Geo-Reconstruct was chosen for volume fraction spatial discretization as it is the most accurate interface-tracking scheme [11]. Spatial discretization of momentum, turbulent dissipation rate and turbulent kinetic energy was achieved by First Order Upwind scheme. A summary of the computational solver and models details is given in Table 4. In these preliminary simulations, all the simulations were run for the same number of time steps of 10,000 with time step size of 0.0001 s.

Table 3. Water and SAE oil viscosity and density values at 20°C [6]

Liquid parameters		
Liquid	Dynamic Viscosity [mPa.s]	Density [kg/m³]
Water	1.02	998.0
SAE 15W-40 Motor Oil	287.23	878.7

From the preliminary post processed results, it was evident that sloshing was more pronounced in water than SAE 15W-40 Motor oil. This can be seen in the air fraction contour images (see Fig. 13) produced at the end of the simulation. The less pronounced sloshing seen in SAE oil as well as the ease to achieve Couette flow earlier than water was attributed to the high viscosity of the oil. The dynamic viscosity of SAE oil is about 280 times that of water while SAE oil density is about 0.88 time that of water. Therefore, the main determinant of the aforementioned differences is viscosity. Other researchers have observed this same influence of viscosity on fluid mechanics in centrifugal casting. Keerthiprasad et al. undertook both numerical simulations and experiments to investigate the influence of liquid viscosity on centrifugal casting [14]. They found out that viscosity played a vital role in the centrifugal casting process - viscous fluid required lower RPM to attain Couette flow, compared to less viscous flow like water. They further noted that sloshing and other phenomena like Ekman flow and turbulence were observed only for low-viscosity fluids like water, these phenomena were negligible in high-viscous liquids like oil.

Table 4. Computational solver and model details

| Input	Value
Analysis Type	Transient Simulation
Gravity	On
Viscous Model	Standard k-epsilon model
Multiphase Model	Volume of Fluid (VOF)
Pressure-Velocity Coupling Scheme	PISO
Spatial Discretization:	
1. Momentum	First Order Upwind
2. Volume Fraction	Geo-Reconstruct
3. Pressure	PRESTO!
4. Turbulent Dissipation Rate	First Order Upwind
5. Turbulent Kinetic Energy	First Order Upwind
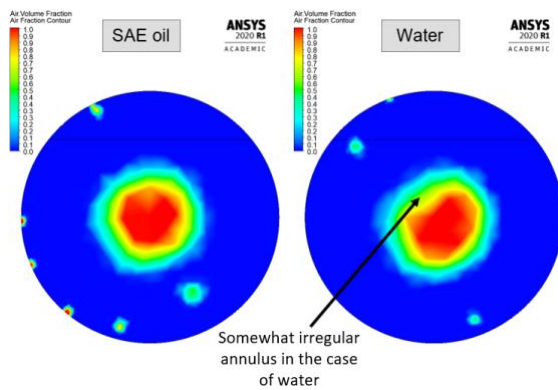
Fig. 13. SAE oil and water air volume fraction contours

Fig. 14 and Fig. 15 further confirm the observation of Keerthiprasad et al.], that high viscous liquids require less RPM to attain Couette flow [14]. SAE oil achieved Couette flow much earlier than water, see for instance in Fig. 14 for the case of 2000 RPM, SAE oil had formed an annulus by time t = 20 s while water took longer time only forming an annulus at around t = 30 s. Furthermore, it was observed that both liquids were unable to form an annulus at 100 RPM. At 1000 RPM, there was a partial annulus formation in SAE oil, water could not form an annulus by the end of the simulation. It should be noted, as aforementioned, all these simulations were run for the same number of time steps of 10,000 with time step size of 0.0001 s.
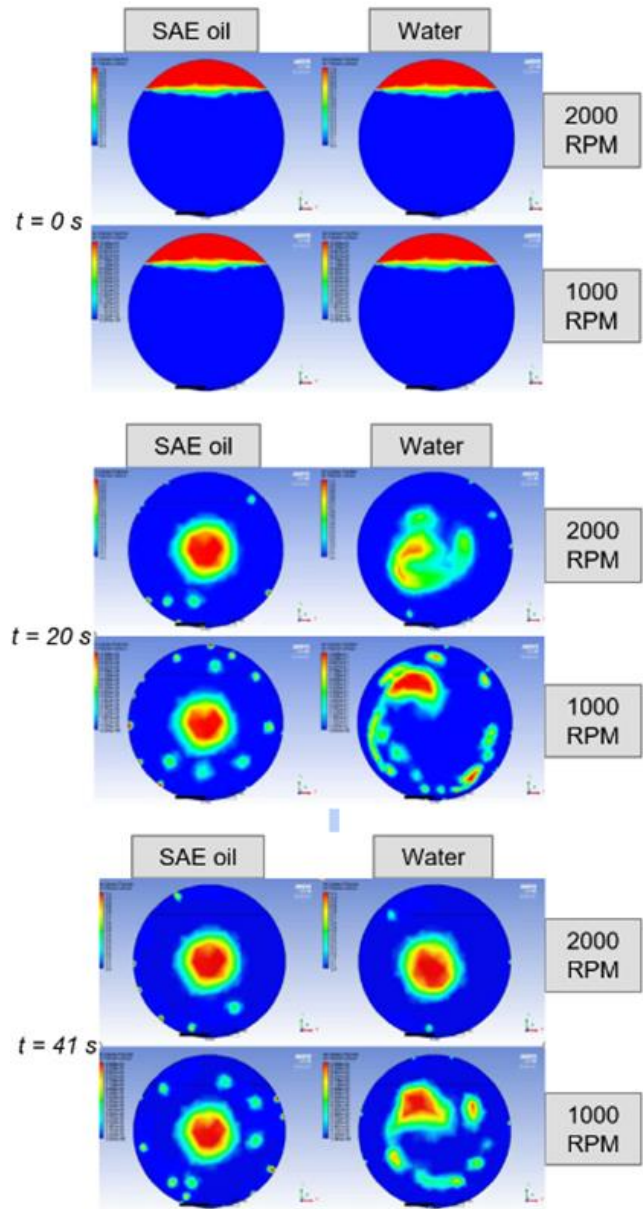
Fig. 14. SAE oil and water air volume fraction contours at different times (t =0 s, 20 s and 41 s) of the simulation for 1000 RPM and 2000 RPM cases
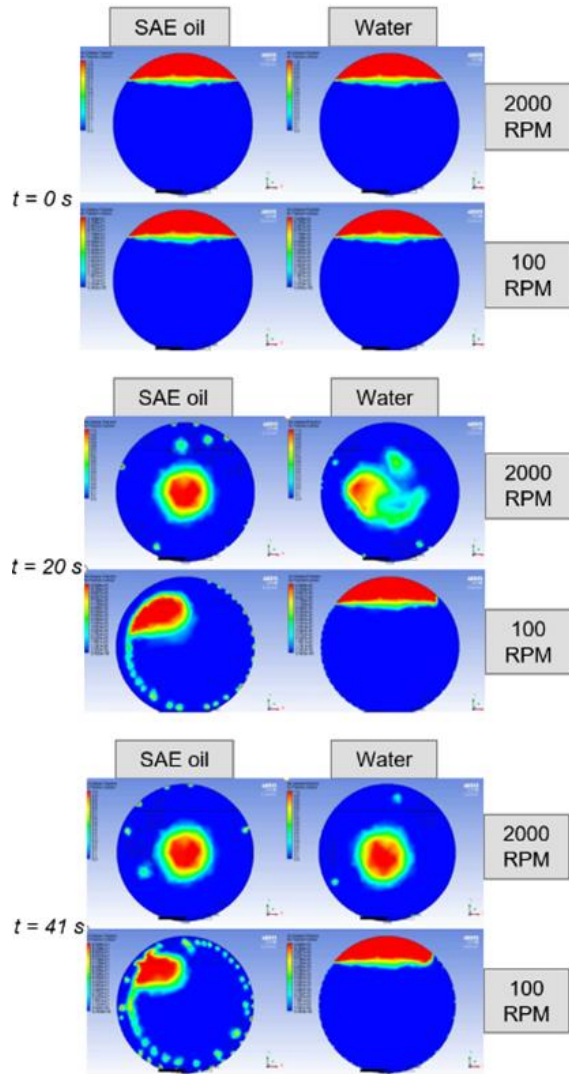
Fig. 15. SAE oil and water air volume fraction contours at different times (t =0 s, 20 s and 41 s) of the simulation for 100 RPM and 2000 RPM cases

The next set of numerical simulations is currently underway. These numerical simulations have been carried out using a much more refined mesh which will enable visualization of finer details of fluid mechanics during centrifugal casting. In addition to water and SAE oil, the ongoing numerical work will investigate paraffin wax fluid mechanics at three different rotational speeds, as shown in Table 2. This set of numerical simulations will offer an insight into the influence of liquid properties, such as density and viscosity, on centrifugal casting.

5. Conclusion

An image analysis routine was developed in order to automate the process of determining the solidification rate of paraffin and beeswax through a side window

during the centrifugal casting process. Beeswax solidified more quickly than paraffin, which suggests that it may be a better working fluid for short-duration microgravity platforms. A rotation rate control device is in the process of development which will be necessary for the constrained experimental environments of suborbital and orbital spaceflight. The device leverages carefully placed magnets to feed rotation rate back into the microcontroller. A modeling effort has begun which seeks to simulate all experimental tests in the lab as well as in microgravity; in standard atmosphere as well as in vacuum. The modeling effort will ultimately include the effects of heat transfer and fluid mechanics on the centrifugal casting process and address the challenges of phase change. Upcoming flights onboard reduced-gravity aircraft, suborbital spacecraft, and -- aspirationally -- an orbital platform will provide higher-fidelity data than the prior experiments.

References
[1] Karabeyoglu, A., Zilliac, G., Cantwell, B.J., DeZilwa, S., and Castellucci, P., "Scale-Up Tests of High Regression Rate Paraffin-Based Hybrid Rocket Fuels," *Journal of Propulsion and Power*, doi: 10.2514/1.3340, 2004
[2] Zilliac, G., Waxman, B., Karabeyoglu, A., Cantwell, B., and Evans, B., "Peregrine Hybrid Rocket Motor Development," *50th AIAA/ASME/SAE/ASEE Joint Propulsion Conference*, doi: 10.2514/6.2014-3870, July 2014, Cleveland, OH
[3] Story, G., Karp, A., Nakazono, B., Zilliac, G., Evans, B., and Whittinghill, G., "Mars Ascent Vehicle Hybrid Propulsion Effort," doi: 10.2514/6.2020-3727, *AIAA/SAE/ASEE Propulsion and Energy Forum*, 24-28 August 2020, Virtual Event
[4] Quinn, G., Steiber, J., Sheth, R., and Ahlstrom, T., Phase Change Material Heat Sink for an ISS Flight Experiment," ICES-2015-167, *45th International Conference on Environmental Systems*, 12-16 July 2015, Bellevue, WA
[5] Stober, K.J., Cantwell, B., and AL Otaibi, R., "Hypergolic Ignition of Lithium--Aluminum--Hydride-

Doped Paraffin Wax and Nitric Acid," doi: 10.2514/1.B37425, 2019, *Journal of Propulsion and Power*, 2019

[6] Stober, K.J., Wanyiri, J., Sanchez, A., Hooper, M., Mazumder, M., Jiwani, S., Waft, C., Lifson, M., Joseph, C., and Wood, D., "An Investigation of the Centrifugal Casting of Paraffin Wax in the Laboratory and in Microgravity," doi: 10.2514/6.2019-4012, *AIAA Propulsion and Energy Forum*, 19-22 August 2019, Indianapolis, IN

[7] Stober, K.J., Wanyiri, J., Sanchez, A., Jiwani, S., Hooper, M., Mazumder, M., Lifson, M., Joseph, C., and Wood, D., "An Investigation of the Laboratory-Based and Microgravity Centrifugal Casting of Paraffin Wax," IAC-19-A2.3.1.52725, *70th International Astronautical Congress*, 21-25 October 2019, Washington, D.C.

[8] Stober, K.J., Sanchez, J., Wanyiri, J., Jiwani, S., and Wood, D., "Centrifugal Casting of Paraffin and Beeswax for Hybrid Rockets," doi: 10.2514/6.2020-3736, *AIAA Propulsion and Energy Forum*, 24-28 August 2020, Virtual Event

[9] Bogdanov, S., "Quality and Standards of Pollen and Beeswax," Apiacta, 38 (2004), pp. 334-341

[10] Krell, R., "Value-Added Products from Beekeeping," FAO Agricultural Services, Bulletin No. 124, Food and Agriculture Organization of the United Nations, Rome, Italy, 1996

[11] Tulloch, A.P., "Beeswax—Composition and Analysis," Bee World, doi: 10.1080/0005772X.1980.11097776, Vol. 61, 1980, Issue 2, pp. 47-62

[12] Blumm, J. and Lindemann, A., "Characterization of the Thermophysical Properties of Molten Polymers and Liquids Using the Flash Technique," High Temperatures – High Pressures, Vol. 35/36, pp. 627-632, 2003/2007, doi: 10.1068/htjr144

[13] Thoroddsen, S. T., and Mahadevan, L., 1997, "Experimental study of coating flows in a partially-filled horizontally rotating cylinder," Experiments in fluids, 23(1), pp. 1-13.

[14] Keerthiprasad, K. S., Murali, M. S., Mukunda, P. G., and Majumdar, S., 2011, "Numerical simulation and cold modeling experiments on centrifugal casting," Metallurgical and materials transactions B, 42(1), pp. 144-155.

[15] Fluent, A., 2013, "ANSYS Fluent Tutorial Guide, Version 15.0," Pennsylvania, US.